Chemistry and Physics of Lipids 164 (2011) 177–183

Contents lists available at ScienceDirect

Chemistry and Physics of Lipids

journal homepage: www.elsevier.com/locate/chemphyslip

Review

Pivotal surfaces in inverse hexagonal and cubic phases of phospholipids and glycolipids

Derek Marsh*

Max-Planck-Institut für biophysikalische Chemie, Am Fassberg 11, 37077 Göttingen, Germany

ARTICLE INFO

Article history:
Received 26 November 2010
Accepted 21 December 2010
Available online 6 January 2011

Keywords:
Non-Lamellar phase
Inverse hexagonal phase
Inverse cubic phase
Spontaneous curvature
Pivotal plane

ABSTRACT

Data on the location and dimensions of the pivotal surfaces in inverse hexagonal (H_{II}) and inverse cubic (Q_{II}) phases of phospholipids and glycolipids are reviewed. This includes the H_{II} phases of dioleoyl phosphatidylethanolamine, 2:1 mol/mol mixtures of saturated fatty acids with the corresponding diacyl phosphatidylcholine, and glucosyl didodecylglycerol, and also the $Q_{II}^{230/G}$ gyroid inverse cubic phases of monooleoylglycerol and glucosyl didodecylglycerol. Data from the inverse cubic phases are largely compatible with those from inverse hexagonal H_{II}-phases. The pivotal plane is located in the hydrophobic region, relatively close to the polar–apolar interface. The area per lipid at the pivotal plane is similar in size to lipid cross-sectional areas found in the fluid lamellar phase (L_α) of lipid bilayers.

Contents

1. Introduction

Lipids with an intrinsic tendency to form nonlamellar phases in aqueous dispersion are characterized by a high spontaneous curvature, $c_o = 1/R_o$. The latter is defined by the radius of curvature, R_p, at the pivotal plane in inverse hexagonal (H_{II}) phases (Leikin et al., 1996). The pivotal plane is the surface at which the area remains constant as the curvature in the H_{II} phase is changed by varying the water content (i.e., $\partial A_p/\partial \bar{c} = 0$). This definition is restricted to this type of experiment and does not correspond to the neutral surface, which is the surface where bending and stretching contributions to the elastic energy are uncoupled, and is a quite general property of the lipid–water system (see Kozlov and Winterhalter, 1991; Leikin et al., 1996). An equivalent definition of pivotal surfaces applies to bicontinuous inverse cubic (Q_{II}) phases that are based on infinite periodic minimal surfaces (IPMS) (Templer, 1995). In this case, the parallel pivotal surfaces of the lipid bilayer are symmetrically displaced from the IPMS.

Pivotal surfaces therefore assume a central role in characterizing the tendency of lipid membranes to form nonlamellar phases, and correspondingly for the functional consequences of curvature frustration on membrane-embedded enzymes and transport systems

* Corresponding author. Tel.: +49 5512011285; fax: +49 5512011501.
E-mail address: dmarsh@gwdg.de

0009-3084/$ – see front matter © 2011 Elsevier Ireland Ltd. All rights reserved.
doi:10.1016/j.chemphyslip.2010.12.010

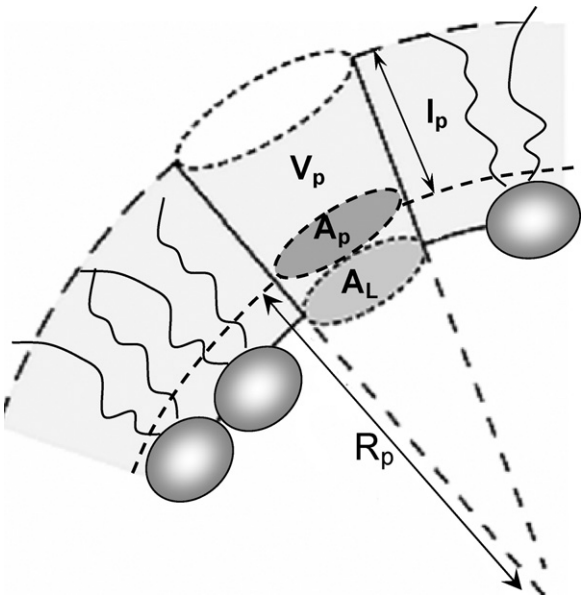

Fig. 1. Position of the pivotal plane (heavy broken lines), relative to the lipid–water interface, in inverse hexagonal (H_{II}) phases. A_p is the area per lipid at the pivotal plane and v_p is the volume per lipid (of total volume v_l) that lies outside the pivotal surface. R_p is the radius of the pivotal surface.

(see, e.g., Marsh, 2007). The purpose of the present communication is to catalogue and compare the pivotal surfaces for the available database of phospholipid and glycolipid inverse hexagonal and cubic phases.

2. Mathematical background

2.1. Pivotal surfaces in inverse hexagonal (H_{II}) phases

Removal of water from an inverse nonlamellar phase increases the surface curvature of the lipid component. The pivotal surface is that plane which maintains constant area as the curvature changes in response to osmotic stress or decreasing water content. The pivotal surface is offset from the lipid–water interface and encloses a volume per lipid, v_p, that is smaller than the total lipid volume, v_l (see Fig. 1). In terms of conventional derivations of the dimensions for inverse phases, which are referred to the lipid–water interface, those for the pivotal surface are obtained similarly by using the reduced lipid volume, v_p, instead of the total lipid volume, v_l, and also the reduced lipid volume fraction $\phi_l(v_p/v_l)$ in place of the total lipid volume fraction, ϕ_l.

The radius of curvature of the pivotal surface in H_{II}-phases is thus given by:

$$R_p = a_H \sqrt{\frac{\sqrt{3}}{2\pi}\left(1 - \frac{v_p}{v_l}\phi_l\right)} \tag{1}$$

where a_H is the hexagonal lattice constant. This expression is determined solely by geometry and applies to any dividing surface. The radius of the lipid–water interface in H_{II}-phases, for instance, is given by substituting $v_p = v_l$ in Eq. (1) (cf. Seddon et al., 1984). The area per lipid at the pivotal surface is correspondingly given by:

$$A_p = \frac{4\pi R_p v_l}{\sqrt{3} a_H^2 \phi_l} \tag{2}$$

Substituting for R_p in Eq. (2) then gives the dependence of the hexagonal lattice constant on water content, $\phi_w = 1 - \phi_l$ (see Templer et al., 1998b):

$$a_H = \frac{2v_l}{A_p\phi_l}\sqrt{\frac{2\pi}{\sqrt{3}}\left(1 - \frac{v_p}{v_l}\phi_l\right)} \tag{3}$$

Hence A_p and v_p, which are independent of water content, may be determined from measurements of the hexagonal lattice constant, a_H, in a swelling experiment. Success in fitting a_H as a function of ϕ_l according to the above expression demonstrates the existence of a well-defined pivotal plane (which must not necessarily be the case for high curvatures – see Leikin et al., 1996).

Having determined the position of the pivotal plane, the radius of curvature of the pivotal surface, R_p, then can be determined from Eq. (1) by using the value of the pivotal lipid volume v_p obtained from the swelling experiments. Eq. (3) can have numerical advantages over the original linearised form introduced in Leikin et al. (1996), in that the parameters of the pivotal surface may be obtained with better precision (cf. Di Gregorio and Mariani, 2005).

2.2. Pivotal surfaces in inverse cubic (Q_{II}) phases

Bicontinuous inverse cubic phases in which both lipid and water components are continuous and constitute a bilayer motif, are based on periodic minimal surfaces. The IPMS defines the midplane of the lipid bilayer, and the pivotal surfaces of each monolayer are displaced from it at a distance l_p.

Minimal surfaces are saddle shaped and the mean curvature is zero everywhere on the surface ($c_1 = -c_2$, and $\bar{c} = 0$). Thus, for each cubic unit cell, the surface area at the pivotal surface is:

$$A_{cell}(l_p) = A_{cell}(0)\left(1 + l_p^2\langle\bar{c}_G^2\rangle\right) \tag{4}$$

where $A_{cell}(0)$ is the area of the minimal surface, per cubic unit cell, and $\langle\bar{c}_G^2\rangle$ is the mean Gaussian curvature of the minimal surface (see, e.g., Marsh, 2006). The mean Gaussian curvature is given from the Gauss–Bonnet theorem by:

$$\langle\bar{c}_G^2\rangle = \frac{2\pi\chi}{A_{cell}(0)} \tag{5}$$

where χ is the Euler characteristic of the surface, per cubic unit cell. Hence the surface area per unit cell of one lipid monolayer is given by (Anderson et al., 1988):

$$A_{cell}(l_p) = \sigma_o a^2 + 2\pi\chi l_p^2 \tag{6}$$

where a is the cubic lattice constant and $\sigma_o = A_{cell}(0)/a^2$ is the dimensionless area per cubic unit cell of the minimal surface. Values of χ and σ_o for the common cubic phases that are based on an IPMS are listed in Table 1.

The area per lipid molecule at the pivotal surface, $A_p = 2A_{cell}(l_p)v_l/(a^3\phi_l)$, is hence given by:

$$A_p = \frac{2v_l}{a\phi_l}\left[\sigma_o + 2\pi\chi\left(\frac{l_p}{a}\right)^2\right] \tag{7}$$

Table 1
Euler characteristic, χ, and dimensionless surface area, σ_o, per unit cell for bicontinuous inverse cubic phases based on infinite periodic minimal surfaces.

Cubic phase	Minimal surface	χ	σ_o
Q_{II}^{224} (Pn3m)	*D*	−2	1.9189
Q_{II}^{229} (Im3m)	*P*	−4	2.3451
Q_{II}^{230} (Ia3d)	*G*	−8	3.0915

The volume per unit cell that is contained between the minimal surface and the pivotal surface is given by:

$$V_{cell}(l_p) = \int_0^{l_p} A_{cell}(z)\,dz = A_{cell}(0) l_p \left(1 + \frac{1}{3} l_p^2 \langle \bar{c}_G^2 \rangle\right) \tag{8}$$

Thus the volume fraction between pivotal and minimal surfaces, $(v_p/v_l)\phi_l = 2V_{cell}(l_p)/a^3$, is given by (Turner et al., 1992):

$$\frac{v_p}{v_l}\phi_l = 2\sigma_o \frac{l_p}{a} + \frac{4\pi}{3}\chi\left(\frac{l_p}{a}\right)^3 \tag{9}$$

Eq. (9) is a cubic equation that has two positive roots ($\phi_l < 1$), the physically realistic of which gives the following solution for the separation of the pivotal surfaces in bicontinuous cubic phases:

$$d_p = 2l_p = a\sqrt{\frac{8\sigma_o}{\pi|\chi|}}\cos\left(\frac{\pi + \vartheta_p}{3}\right),$$

$$\text{where} \quad \cos\vartheta_p = \phi_l \frac{v_p}{v_l}\sqrt{\frac{9\pi|\chi|}{8\sigma_o^3}} \tag{10}$$

This is determined solely by the water content of the phase, $\phi_w = 1 - \phi_l$, and the cubic lattice constant, a. The lipid bilayer thickness, d_l, and the area per lipid at the lipid–water interface, A_w, can be obtained in a similar way by using the full lipid length, l_l, that is deduced from Eq. (10) with $v_p = v_l$.

Substituting for l_p/a from Eq. (10) in the expression for A_p (Eq. (7)) then gives the following dependence of the cubic lattice constant on the water (or lipid) content of the cubic phase:

$$a = \frac{2\sigma_o v_l}{A_p \phi_l}\left[1 - 4\cos^2\left(\frac{\pi + \vartheta_p}{3}\right)\right] \tag{11}$$

where ϑ_p depends on ϕ_l and v_p according to the second part of Eq. (10). As in the case of H_{II}-phases, A_p and v_p can thus be determined from the dependence of the lattice constant a on ϕ_l in a swelling experiment. Values for the separation, d_p, of the pivotal planes then follow by using these determinations of v_p.

3. Inverse hexagonal (H_{II}) phases of phospholipids and glycolipids

3.1. Phosphatidylethanolamines

The dependence of the hexagonal lattice constant on water content of the dioleoyl phosphatidylethanolamine H_{II}-phase at 22 °C is shown in the upper panel of Fig. 2 (Rand et al., 1990; Gruner et al., 1986). Up to the maximum hydration at a water/lipid ratio of $n_w = 19$ mol/mol, the dependence of a_H on n_w is well fit by Eq. (3). The lipid volume fraction is:

$$\phi_l = \frac{1}{1 + (v_w/v_l)n_w} \tag{12}$$

where v_w is the volume of a water molecule. The nonlinear least-squares fit yields the following optimized parameters: $v_p/v_l = 0.604 \pm 0.024$ and $A_p/v_l = 0.578 \pm 0.011\,\text{nm}^{-1}$ at 22 °C. For a molecular volume of $v_l = 1.215\,\text{nm}^3$ (Tate and Gruner, 1989), this yields an area per lipid at the pivotal plane of: $A_p = 0.703 \pm 0.014\,\text{nm}^2$.

The lower panel of Fig. 2 contrasts the dependence on water content of the area per lipid at the pivotal plane (A_p) with that at the lipid/water interface (A_w). A_p remains constant, as it must for a well-defined pivotal plane, whereas A_w increases steeply with increasing water content up to the point of maximum hydration. A_p is greater than A_w, and correspondingly for the radii R_p and R_w of

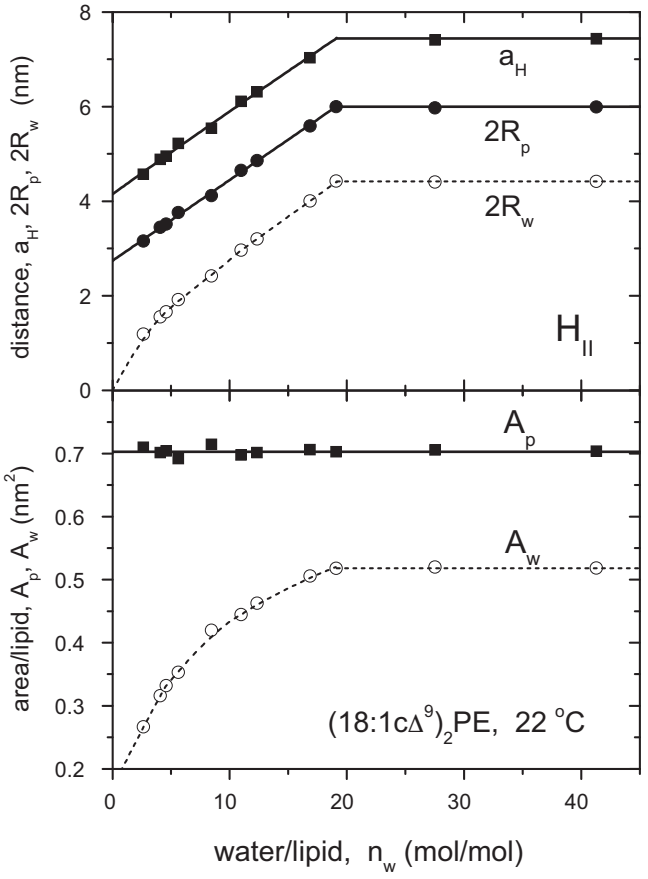

Fig. 2. Dependence on water/lipid ratio, n_w, of: (*upper panel*) the hexagonal lattice constant, a_H, the cylinder radii of the pivotal surface (R_p) and lipid–water interface (R_w), and (*lower panel*) the areas per lipid at the pivotal surface (A_p) and lipid–water interface (A_w), for the inverse hexagonal (H_{II}) phase of 1,2-dioleoyl-*sn*-glycero-3-phosphoethanolamine at 22 °C. Data from Rand et al. (1990); Gruner et al. (1986). The solid line for a_H at $n_w \leq 19$ is a nonlinear, least-squares fit of Eq. (3) (with Eq. (12)) for the pivotal plane.

the pivotal plane and lipid–water interface, respectively, indicating that the pivotal plane lies inside the lipid region (because $v_p < v_l$).

At excess water, the radius of the pivotal plane in the H_{II}-phase is the spontaneous radius of curvature, $R_{o,p}$, that specifies the intrinsic propensity of the lipid assembly to bend (see, e.g., Marsh, 1996, 2006). For lipids with low intrinsic curvature that do not form H_{II} phases spontaneously, these can be induced by addition of excess liquid alkane, which alleviates the chain packing frustration that is inherent to the hexagonal phase geometry (Gruner, 1985).

Table 2 gives the dimensions of the H_{II}-phase for phosphatidylethanolamines, including those of the pivotal plane. The temperature dependence for dioleoyl phosphatidylethanolamine, $(18:1c\Delta^9)_2$PE, is deduced from the data of Tate and Gruner (1989), with additional data at 22 °C from Rand et al. (1990) and Rand and Fuller (1994). An aggregate pivotal volume of $v_p \approx 0.79\,\text{nm}^3$ is obtained for $(18:1c\Delta^9)_2$PE at 20–25 °C. Taking a volume per CH_2 group of $0.027\,\text{nm}^3$ and ratios of volumes $CH_3/CH_2 = 2$ and $CH/CH_2 = 0.85$ (Marsh, 2010), the pivotal plane is predicted to lie in the region of the C4–C5 atom of the chains. A similar calculation for $(20:0)_2$PE at 99 °C, for which the pivotal volume is $v_p = 1.18 \pm 0.05\,\text{nm}^3$, puts the pivotal plane close to the chain carbonyls. For the shorter ether-linked $(O\text{-}12:0)_2$PE at 135 °C, on the other hand, the pivotal volume is predicted to be $v_p = 0.11 \pm 0.09\,\text{nm}^3$ and the volume per CH_2 group is $0.0286\,\text{nm}^3$, which implies that the pivotal plane is situated close to the terminal methyl groups. This latter is an unphysical result, which arises because packing frustration becomes dominant relative to curvature energy in the

Table 2
Dimensions at the pivotal plane and lipid–water interface for H_{II}-phases of phosphatidylethanolamines in excess water.

Lipid	T (°C)	n_w^{max} (mol/mol)	$R_{o,p}$ (nm)	R_w (nm)	A_p[a] (nm^2)	A_w (nm^2)	v_p/v_l[a]	Ref.[b]
$(18:1c\Delta^9)_2$PE	10	18.0	3.78	2.28	0.785 ± 0.029	0.473	0.215 ± 0.086	1
	15	17.5	3.42	2.21	0.732 ± 0.017	0.474	0.399 ± 0.044	1
	20	16.9	2.91	2.15	0.639 ± 0.016	0.471	0.650 ± 0.034	1
	20	19.5	3.06	2.26	0.698 ± 0.003	0.506	0.616 ± 0.005	2
	22	19.1	3.00	2.21	0.703 ± 0.014	0.518	0.604 ± 0.024	3,4
	22	20.3	3.10	2.26	0.729 ± 0.013	0.539	0.562 ± 0.027	4
	22	18.1	2.89	2.16	0.663 ± 0.008	0.502	0.649 ± 0.015	5
	25	16.6	2.84	2.10	0.643 ± 0.016	0.475	0.659 ± 0.033	1
	30	16.2	2.78	2.05	0.646 ± 0.020	0.476	0.665 ± 0.040	1
	35	16.0	2.73	2.00	0.655 ± 0.021	0.480	0.663 ± 0.041	1
	40	15.6	2.62	1.95	0.642 ± 0.019	0.479	0.697 ± 0.037	1
	45	15.2	2.53	1.91	0.634 ± 0.019	0.478	0.719 ± 0.035	1
	50	14.9	2.45	1.86	0.630 ± 0.021	0.480	0.738 ± 0.035	1
	55	14.7	2.42	1.83	0.637 ± 0.022	0.483	0.735 ± 0.037	1
	60	14.5	2.30	1.79	0.645 ± 0.024	0.485	0.774 ± 0.039	1
	65	14.2	2.28	1.75	0.633 ± 0.025	0.486	0.763 ± 0.039	1
	70	14.0	2.22	1.72	0.630 ± 0.020	0.488	0.776 ± 0.031	1
	75	13.8	2.17	1.68	0.633 ± 0.018	0.491	0.782 ± 0.028	1
	80	13.7	2.16	1.66	0.645 ± 0.018	0.495	0.773 ± 0.032	1
	85	13.7	2.13	1.64	0.650 ± 0.020	0.500	0.777 ± 0.029	1
	90	13.6	2.13	1.62	0.663 ± 0.029	0.505	0.767 ± 0.043	1
$(20:0)_2$PE	99	15.7	2.53	2.11	0.557 ± 0.033	0.464	0.845 ± 0.038	6
$(O\text{-}12:0)_2$PE	135	15.8	(2.64)[c]	1.60	(1.04 ± 0.04)[c]	0.632	(0.114 ± 0.09)[c]	6

[a] Deduced from the water dependence.
[b] References: 1. Tate and Gruner (1989); 2. Di Gregorio and Mariani (2005); 3. Gruner et al. (1986); 4. Rand et al. (1990); 5. Rand and Fuller (1994); 6. Seddon et al. (1984).
[c] Packing stresses dominate over bending elasticity, making estimation of the pivotal plane inaccurate (see text).

high-temperature H_{II}-phases of this short-chain lipid. Comparison with the result for long-chain $(20:0)_2$PE suggests, however, that the pivotal plane moves outwards, deeper into the hydrocarbon region, with decreasing chain length.

Fig. 3 compares the temperature dependences of the dimensions of the pivotal plane (solid symbols) for the H_{II}-phase of $(18:1c\Delta^9)_2$PE with those for the lipid–water interface (open symbols). The area per lipid (A_w) and radius (R_w) at the lipid–water interface, and the total lipid volume (v_l), vary smoothly with temperature (see also Tate and Gruner, 1989). In contrast, the area per lipid (A_p) and radius (R_p) of the pivotal plane, and the pivotal lipid volume (v_p), change rapidly between 10 and 20 °C before assuming a less steep temperature dependence. These sharp initial changes are probably a feature of the low-temperature region close to 0 °C, where the lipid chains are stiffer and the packing stresses that arise from the nonuniform radial geometry of the H_{II}-phase dominate over the bending stresses. At higher temperatures, the chains are more flexible, packing stresses are less important, and the free energy is dominated by bending elasticity. The data in the lower panel of Fig. 3 are of particular interest, because the temperature dependence of the spontaneous radius of curvature ($R_{o,p}$, solid triangles) of the pivotal surface for $(18:1c\Delta^9)_2$PE has not been reported previously, only that of the lipid–water interface ($R_{o,w}$) (Tate and Gruner, 1989). The pressure dependence of the spontaneous curvature at the pivotal plane is reported for $(18:1c\Delta^9)_2$PE by Pisani et al. (2003).

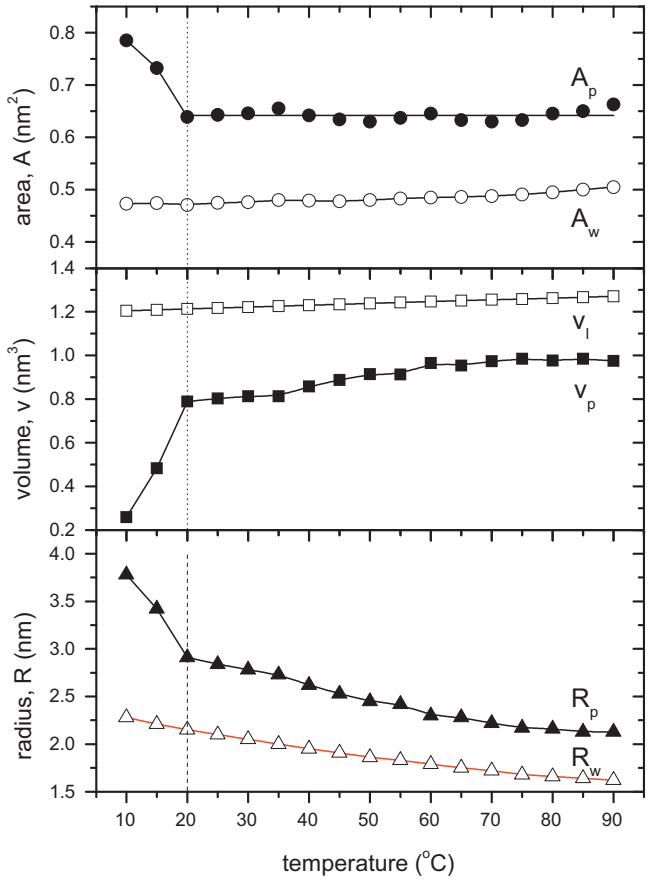

Fig. 3. Dependence on temperature of the properties of the pivotal surface (solid symbols) and lipid–water interface (open symbols) for the H_{II}-phase of $(18:1c\Delta^9)_2$PE. *Top panel*: area per lipid at the pivotal surface (A_p, solid circles), and at the lipid–water interface (A_w, open circles). *Middle panel*: pivotal lipid volume (v_p, solid squares), and total lipid volume (v_l, open squares). *Bottom panel*: radius of the pivotal surface (R_p, solid triangles), and of the lipid–water interface (R_w, open triangles). Primary data from Tate and Gruner (1989).

3.2. Lipid mixtures

Table 3 gives the dependence on lipid chain length of the dimensions of the H_{II}-phases that are formed by 1:2 mol/mol mixtures of disaturated phosphatidylcholines with fatty acids of the corresponding chain lengths. The fatty acids are in the protonated (uncharged) state and thus have a strong tendency to form inverted phases on admixture with phosphatidylcholines (Marsh and Seddon, 1982; Rama Krishna and Marsh, 1990; Heimburg et al., 1990). Data are given at a temperature that is 10 ° above the transition to the H_{II}-phase for the respective chain lengths. The parameters of the pivotal planes for these mixtures were presented

Table 3
Dimensions at the pivotal plane and lipid–water interface for H_{II} phases of phosphatidylcholine:fatty acid 1:2 mol/mol mixtures with matched saturated chains in excess water.

Lipid	T (°C)	n_w^{max} [a] (mol/mol)	$R_{o,p}$ (nm)	R_w (nm)	A_p [a,b] (nm^2)	A_w [a] (nm^2)	v_p/v_l [b]	Ref.[c]
$(12:0)_2$PC/(12:0)FA 1:2 mol/mol	40	10.5	2.14	1.56	0.553 ± 0.015	0.403	0.681 ± 0.029	1
$(14:0)_2$PC/(14:0)FA 1:2 mol/mol	60	9.6	2.10	1.48	0.562 ± 0.015	0.474	0.693 ± 0.023	1
$(16:0)_2$PC/(16:0)FA 1:2 mol/mol	70	14.1	2.39	1.93	0.546 ± 0.026	0.441	0.789 ± 0.035	2
$(18:0)_2$PC/(18:0)FA 1:2 mol/mol	80	13.8	2.29	1.82	0.574 ± 0.027	0.456	0.794 ± 0.033	2
$(20:0)_2$PC/(20:0)FA 1:2 mol/mol	90	13.5	2.30	1.78	0.586 ± 0.029	0.453	0.795 ± 0.033	2

Note: the fatty acid is protonated.
[a] Value per *two* chains.
[b] Deduced from water dependence.
[c] References: 1. Templer et al. (1998b); 2. Seddon et al. (1997).

in the original study by Templer et al. (1998b). The present evaluations, which are mean values per two chains instead of for the 1:2 complex, agree with those values.

It was found by Templer et al. (1998b) that the location of the pivotal plane and its area does not change with chain length for the 1:2 mol/mol phosphatidylcholine–fatty acid mixtures. This is illustrated in Fig. 4, which shows the dependence of v_p and A_p on lipid chain length, n_C. The difference between v_l, the total lipid molecular volume, and v_p remains essentially constant, as does the value of A_p, for the different chain lengths. Estimates based on a methylene group volume of 0.027 nm^3 place the pivotal plane in the region of the C2 atom of the chains for each system.

3.3. Glycosyl dialkylglycerols

Fig. 5 shows the dependence of the H_{II}-phase dimensions on water content for a glycolipid system, monoglucosyl didodecylglycerol (*rac*-(O-12:0)$_2$GlcβDG). This is exactly comparable to the data for dioleoyl phosphatidylethanolamine in Fig. 2. The maximum hydration ($n_w \approx 12$ mol/mol) is less for the glycolipid than for the phospholipid, and the dimensions of the H_{II}-phase are correspondingly smaller. Table 4 gives the H_{II}-phase dimensions, including those of the pivotal plane, for three temperatures in the H_{II}-regime. The volume of a CH_2 group in the H_{II} phase of glucosyl dialkylglycerols is 0.0265 nm^3 (Marsh, 2010) and the pivotal volume is 0.586 nm^3 at 80 °C. This places the pivotal plane in the region of the C2–C3 atom of the alkyl chains.

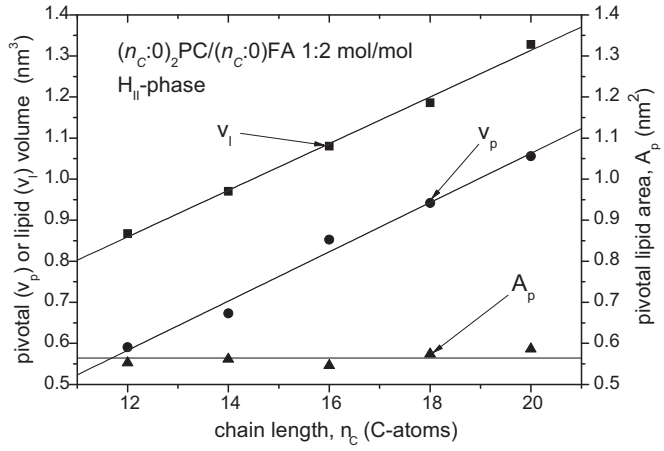

Fig. 4. Chain-length dependence of the pivotal volume (v_p, circles) and surface area (A_p, triangles), per two lipid chains, in the H_{II}-phase from 1:2 mol/mol mixtures of saturated diacyl phosphatidylcholines with the corresponding fatty acid. Data from Table 3. The lipid molecular volume per two chains, v_l, is given by the squares (Templer et al., 1998b). Sloping lines are linear regressions.

4. Inverse cubic (Q_{II}) phases of monoglycerides, phospholipids and glycolipids

4.1. Monoacylglycerols

Fig. 6 shows the dependence on water content, n_w, of the cubic lattice constants, a, for the $Q_{II}^{230/G}$ (Ia3d) gyroid inverse cubic phase of monooleoylglycerol, (18:1cΔ^9/0:0)MG, at 25 °C (Chung and Caffrey, 1994). The dependence is reasonably well fit by Eq. (11), yielding the optimized parameters: $v_p/v_l = 0.582 \pm 0.062$ and $A_p/v_l = 0.574 \pm 0.011$ nm^{-1} for the pivotal surface. With a molecular volume of $v_l = 0.6285$ nm^3 (based on the density at 20 °C), this gives an area per lipid of: $A_p = 0.361 \pm 0.007$ nm^2 at the pivotal plane at 25 °C. Table 5 gives the temperature dependence of the dimensions for the gyroid $Q_{II}^{230/G}$ cubic phase of (18:1cΔ^9/0:0)MG that is deduced from the dependence on water content.

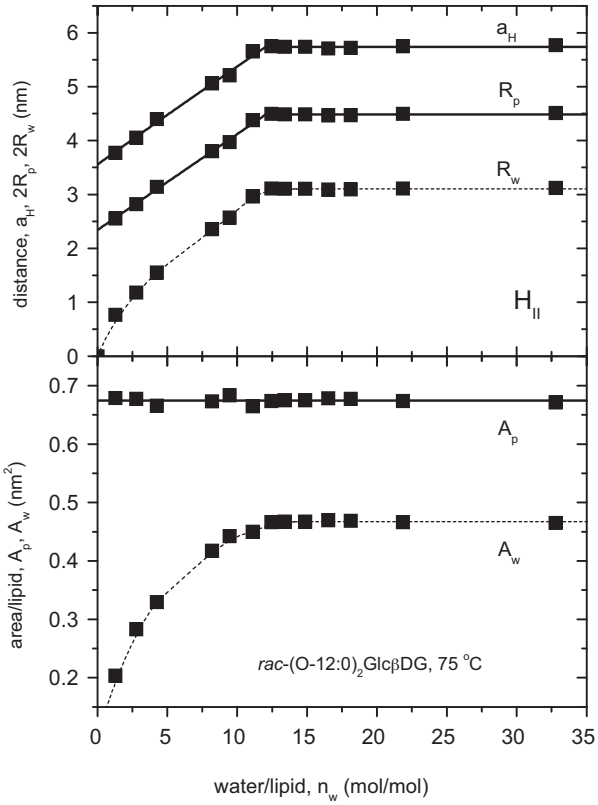

Fig. 5. Dependence on water/lipid ratio, n_w, of: (*upper panel*) the hexagonal lattice constant, a_H, the cylinder radii of the pivotal surface (R_p) and lipid–water interface (R_w), and (*lower panel*) the areas per lipid at the pivotal surface (A_p) and lipid–water interface (A_w), for the inverse hexagonal (H_{II}) phase of *rac*-didodecyl-β-D-glucosylglycerol at 75 °C. Data from Turner et al. (1992). The solid line for a_H at $n_w \leq 12$ is a nonlinear, least-squares fit of Eq. (3) (with Eq. (12)) for the pivotal plane.

Table 4
Dimensions of the pivotal plane and lipid–water interface for the H_{II}-phase of β-D-glucosyl didodecyl-*rac*-glycerol in excess water[a].

T (°C)	$n_w{}^{max}$ (mol/mol)	$R_{o,p}$ (nm)	R_w (nm)	A_p[b] (nm^2)	A_w (nm^2)	v_p/v_l[b]
75	12.1	2.24	1.55	0.674 ± 0.016	0.467	0.607 ± 0.029
80	11.9	2.24	1.51	0.701 ± 0.034	0.471	0.582 ± 0.060
85	12.0	2.23	1.49	0.721 ± 0.038	0.482	0.562 ± 0.068

[a] Data from Turner et al. (1992).
[b] Deduced from water dependence.

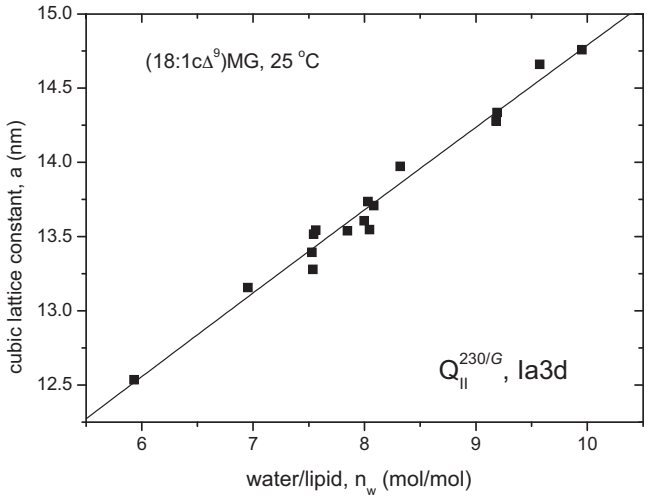

Fig. 6. Dependence of the cubic lattice parameter, a, on water/lipid ratio, n_w, for 1-oleoyl-*sn*-glycerol, (18:1cΔ^9/0:0)MG, in the $Q_{II}{}^{230/G}$ (Ia3d) gyroid cubic phase at 25 °C. Data from Chung and Caffrey (1994). Solid line is a nonlinear, least-squares fit of Eq. (11) (with Eq. (12)) for the pivotal plane relative to the IPMS.

Note that, although the $Q_{II}{}^{224/D}$ (Pn3m) diamond inverse cubic phase occurs in (18:1cΔ^9/0:0)MG, a realistic location for the pivotal surface has been found only when this phase is stabilized by high concentrations of saccharides (Pisani et al., 2001; Saturni et al., 2001). Presumably, in the absence of sugars, packing stresses and/or stretching elasticity are more important than curvature elasticity for the stability of the $Q_{II}{}^{224/D}$ (Pn3m) structure (see also discussion of (O-12:0)$_2$PE in Section 3.1).

4.2. Lipid mixtures

Table 6 gives the dimensions for the pivotal surfaces of the different inverse cubic phases, $Q_{II}{}^{230/G}$ (Ia3d), $Q_{II}{}^{229/P}$ (Im3m) and $Q_{II}{}^{224/D}$ (Pn3m), that are formed by a dilauroyl phosphatidylcholine:lauric acid 1:2 mol/mol mixture (Templer et al., 1998b). These values are determined from the dependence of the cubic lattice parameters on water content (Eq. (11)). As was assumed in the original work (Templer et al., 1998b), the parameters of the pivotal surfaces are found to be similar to those for the inverse hexagonal phase of this lipid mixture, for all three different inverted cubic phases. However, the volume ratio, v_p/v_l, is not determined with great precision for the cubic phases.

Also included in Table 6 are data for the $Q_{II}{}^{230/G}$ gyroid cubic phase of a monooleoylglycerol/dioleoyl phosphatidylcholine/dioleoyl phosphatidylethanolamine 58:38:4 mol/mol/mol ternary mixture (Templer et al., 1998a). The mean pivotal area and volume, per two chains, are close to the weighted average of these values for the individual components, as demonstrated directly by Templer et al. (1998a). At the same temperature, the mean pivotal volume per two chains is close to that for the H_{II}-phase of (18:1cΔ^9)$_2$PE, which has a similar chain composition. Thus the pivotal plane for the mixture is also expected to be located approximately between the C4 and C5 atoms of the chains (cf. above for H_{II}-phases).

Table 5
Dimensions of the pivotal plane and lipid–water interface for the $Q_{II}{}^{230/G}$ (Ia3d) inverse cubic phase of (18:1cΔ^9/0:0)MG deduced from the water dependence.

T (°C)	A_p (nm^2)	v_p/v_l	Ref.[a]
25	0.361 ± 0.007	0.582 ± 0.062	1
	0.370	0.56	2,3
30	0.363 ± 0.013	0.551 ± 0.108	4
50	0.319 ± 0.010	0.833 ± 0.036	4
70	0.322 ± 0.007	0.905 ± 0.019	4

Note: A constant lipid volume of $v_l = 0.6285$ nm^3 was assumed from the density of (18:1cΔ^9/0:0)MG at 20 °C.
[a] References: 1. Chung and Caffrey (1994); 2. Pisani et al. (2001); 3. Mariani et al. (1988); 4. Briggs et al. (1996).

4.3. Glycosyl dialkylglycerols

Fig. 7 shows the dependence on water content, n_w, of the cubic lattice constant for the $Q_{II}{}^{230/G}$ (Ia3d) inverse cubic phase of the glycolipid monoglucosyl didodecylglycerol (*rac*-(O-12:0)$_2$GlcβDG) at 45 °C (Turner et al., 1992). The dependence is adequately fit by Eq. (11), yielding optimized parameters: $v_p/v_l = 0.805 \pm 0.042$ and $A_p/v_l = 0.568 \pm 0.016$ nm^{-1} for the pivotal surface at 45 °C. With a molecular volume of $v_l = 0.980$ nm^3 (Turner et al., 1992), this gives an area per lipid at the pivotal plane of: $A_p = 0.556 \pm 0.016$ nm^2. Table 7 lists the dimensions of the gyroid inverse cubic phase of *rac*-(O-12:0)$_2$GlcβDG as a function of temperature. The pivotal volumes are larger than those in the H_{II}-phase (cf. Table 4) and, in consequence, the pivotal plane is predicted to lie within the region of the polar–apolar interface.

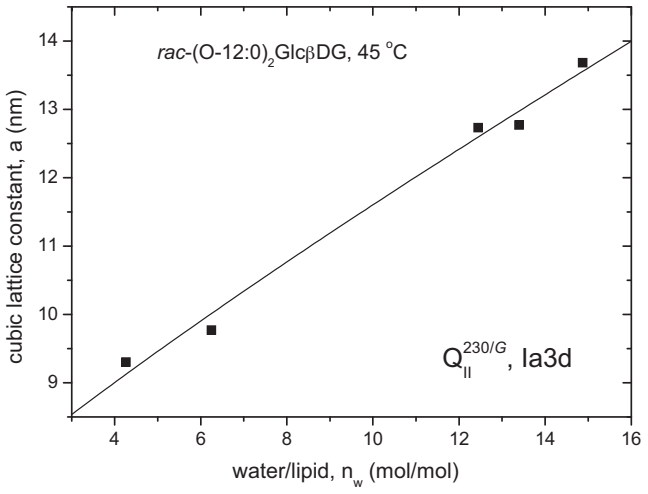

Fig. 7. Dependence of the cubic lattice parameter, a, on water/lipid ratio, n_w, for the $Q_{II}{}^{230/G}$ (Ia3d) gyroid inverse cubic phase of *rac*-didodecyl-β-D-glucosylglycerol at 45 °C. Data from Turner et al. (1992). Solid line is a nonlinear, least-squares fit of Eq. (11) (with Eq. (12)) for the pivotal plane relative to the IPMS.

Table 6
Dimensions of the pivotal plane and lipid–water interface for different inverse cubic phases of dilauroyl phosphatidylcholine:lauric acid 1:2 mol/mol mixture, and of an oleoylglycerol:dioleoyl phosphatidylcholine:dioleoyl phosphatidylethanolamine mixture, deduced from the water dependence.

Lipid	Phase	T (°C)	A_p (nm^2)[a]	v_p/v_l	v_l (nm^3)[a]	Ref.[b]
(12:0)$_2$PC/(12:0)FA 1:2 mol/mol[c]	$Q_{II}^{230/G}$ (Ia3d)	35–45	0.538 ± 0.018	0.855 ± 0.107	0.8675	1
	$Q_{II}^{229/P}$ (Im3m)	35–45	0.551 ± 0.053	–	0.8675	1
	$Q_{II}^{224/D}$ (Pn3m)	35–45	0.527 ± 0.057	0.889 ± 0.352	0.8675	1
(18:1cΔ^9)MG/(18:1cΔ^9)$_2$PC/(18:1cΔ^9)$_2$PE 58:38:4 mol/mol	$Q_{II}^{230/G}$ (Ia3d)	25	0.595 ± 0.011	0.748 ± 0.092	1.0190	2

[a] Mean value per *two* chains.
[b] References: 1. Templer et al. (1998b); 2. Templer et al. (1998a).
[c] The fatty acid is protonated.

Table 7
Dimensions of the pivotal plane for the $Q_{II}^{230/G}$ (Ia3d) inverse cubic phase of β-D-glucosyl didodecyl-*rac*-glycerol, deduced from the water dependence[a].

T (°C)	A_p (nm^2)	v_p/v_l	v_l (nm^3)
45	0.556 ± 0.016	0.805 ± 0.042	0.980
50	0.549 ± 0.013	0.801 ± 0.097	0.984
55	0.570 ± 0.063	0.771 ± 0.156	0.987
60	0.589 ± 0.035	0.744 ± 0.095	0.991

[a] Data from Turner et al. (1992).

5. Conclusion

Whereas the results for the inverse cubic phases (Figs. 6 and 7 and Tables 5–7) support a similar interpretation of the pivotal plane in terms of bending elasticity as that in inverse hexagonal phases, the parameters of the pivotal plane are determined with better precision from the H_{II}-phases than from the Q_{II}-phases. In all cases, the pivotal plane in the inverse phase is situated below the polar–apolar interface, in the hydrocarbon chain region of the lipid (i.e., $v_p < v_l$ in all cases). Depending on the lipid system, the pivotal plane is estimated to lie in the C1 to C4–C5 region of the lipid chains. Judging from the profile of segmental order parameters in H_{II}-phases (Sankaram and Marsh, 1989), this corresponds to the region of least flexibility and closest packing of the lipid chains.

The area per two-chain lipid molecule at the pivotal surface depends on the lipid system, but lies more or less in the range found for the fluid lamellar (L_α) phase of bilayer-forming lipids (cf. Marsh, 1990). For (18:1cΔ^9)$_2$PE, the molecular area at the pivotal surface is almost independent of temperature, when the chains are flexible and packing restraints are no longer dominant. For the phosphatidylcholine:fatty acid 1:2 mixtures, the lipid area at the pivotal surface is essentially independent of lipid chain length, at least when the measurement temperature is adjusted relative to that of chain melting.

These results define broad expectations with respect to pivotal surfaces in lipid systems and emphasise that it is the pivotal surface, and not the lipid–water interface, that is relevant in defining curvature elasticity and spontaneous curvature of lipid systems.

Acknowledgment

I gratefully acknowledge Christian Griesinger and the Dept. for NMR-based structural biology for financial support.

References

Anderson, D., Gruner, S., Leibler, S., 1988. Geometrical aspects of the frustration in the cubic phases of lyotropic liquid crystals. Proc. Natl. Acad. Sci. U.S.A. 85, 5364–5368.
Briggs, J., Chung, H., Caffrey, M., 1996. The temperature-composition phase diagram and mesophase structure characterization of the monoolein/water system. J. Phys. II France 6, 723–751.
Chung, H., Caffrey, M., 1994. The neutral area surface of the cubic mesophase: location and properties. Biophys. J. 66, 377–381.
Di Gregorio, G.M., Mariani, P., 2005. Rigidity and spontaneous curvature of lipidic monolayers in the presence of trehalose: a measurement in the DOPE inverted hexagonal phase. Eur. Biophys. J. Biophys. Lett. 34, 67–81.
Gruner, S.M., 1985. Intrinsic curvature hypothesis for biomembrane lipid composition: a role for non-bilayer lipids. Proc. Natl. Acad. Sci. U.S.A. 82, 3665–3669.
Gruner, S.M., Parsegian, V.A., Rand, R.P., 1986. Directly measured deformation energy of phospholipid H_{II} hexagonal phases. Faraday Discuss. Chem. 81, 29–37.
Heimburg, T., Ryba, N.J.P., Würz, U., Marsh, D., 1990. Phase transition from a gel to a fluid phase of cubic symmetry in dimyristoylphosphatidylcholine/myristic acid (1:2, mol/mol) bilayers. Biochim. Biophys. Acta 1025, 77–81.
Kozlov, M.M., Winterhalter, M., 1991. Elastic moduli and neutral surface for strongly curved monolayers. Position of the neutral surface. J. Phys. II 1, 1077–1084.
Leikin, S., Kozlov, M.M., Fuller, N.L., Rand, R.P., 1996. Measured effects of diacylglycerol on structural and elastic properties of phospholipid membranes. Biophys. J. 71, 2623–2632.
Mariani, P., Luzzati, V., Delacroix, H., 1988. Cubic phases of lipid-containing systems – structure analysis and biological implications. J. Mol. Biol. 204, 165–188.
Marsh, D., 1990. Handbook of Lipid Bilayers. CRC Press, Boca Raton, FL.
Marsh, D., 1996. Intrinsic curvature in normal and inverted lipid structures and in membranes. Biophys. J. 70, 2248–2255.
Marsh, D., 2006. Elastic curvature constants of lipid monolayers and bilayers. Chem. Phys. Lipids 144, 146–159.
Marsh, D., 2007. Lateral pressure profile, spontaneous curvature frustration, and the incorporation and conformation of proteins in membranes. Biophys. J. 93, 3884–3899.
Marsh, D., 2010. Molecular volumes of phospholipids and glycolipids in membranes. Chem. Phys. Lipids 163, 667–677.
Marsh, D., Seddon, J.M., 1982. Gel-to-inverted hexagonal (L_β-H_{II}) phase transitions in phosphatidylethanolamines and fatty acid-phosphatidylcholine mixtures, demonstrated by ^{31}P NMR spectroscopy and X-ray diffraction. Biochim. Biophys. Acta 690, 117–123.
Pisani, M., Bernstorff, S., Ferrero, C., Mariani, P., 2001. Pressure induced cubic-to-cubic phase transition in monoolein hydrated system. J. Phys. Chem. B 105, 3109–3119.
Pisani, M., Narayan, P., Di Gregorio, G.M., Ferrero, C., Finet, S., Mariani, P., 2003. Compressing inverse lyotropic systems: structural behavior and energetics of dioleoyl phosphatidyl ethanolamine. Phys. Rev. E 68, 021924-1–021924-11.
Rama Krishna, Y.V.S., Marsh, D., 1990. Spin label ESR and ^{31}P-NMR studies of the cubic and inverted hexagonal phases of dimyristoylphosphatidylcholine/myristic acid (1:2, mol/mol) mixtures. Biochim. Biophys. Acta 1024, 89–94.
Rand, R.P., Fuller, N.L., 1994. Structural dimensions and their changes in a reentrant hexagonal-lamellar transition of phospholipids. Biophys. J. 66, 2127–2138.
Rand, R.P., Fuller, N.L., Gruner, S., Parsegian, V.A., 1990. Membrane curvature, lipid segregation, and structural transitions for phospholipids under dual-solvent stress. Biochemistry 29, 76–87.
Sankaram, M.B, Marsh, D., 1989. Chain order profile in H_{II} phases. Biophys. J. 56, 1043–1044.
Saturni, L., Rustichelli, F., Di Gregorio, G.M., Cordone, L., Mariani, P., 2001. Sugar-induced stabilization of the monoolein Pn3m bicontinuous cubic phase during dehydration. Phys. Rev. E 64, 040902-1–040902-4.
Seddon, J.M., Cevc, G., Kaye, R.D., Marsh, D., 1984. X-ray diffraction study of the polymorphism of hydrated diacyl- and dialkylphosphatidylethanolamines. Biochemistry 23, 2634–2644.
Seddon, J.M., Templer, R.H., Warrender, N.A., Huang, Z., Cevc, G., Marsh, D., 1997. Phosphatidylcholine–fatty acid membranes: effects of headgroup hydration on the phase behaviour and structural parameters of the gel and inverse hexagonal (H_{II}) phases. Biochim. Biophys. Acta 1327, 131–147.
Tate, M.W., Gruner, S., 1989. Temperature dependence of the structural dimensions of the inverted hexagonal (H_{II}) phase of phosphatidylethanolamine-containing membranes. Biochemistry 28, 4245–4253.
Templer, R.H., 1995. On the area neutral surface of inverse bicontinuous cubic phases of lyotropic liquid-crystals. Langmuir 11, 334–340.
Templer, R.H., Khoo, B.J., Seddon, J.M., 1998a. Gaussian curvature modulus of an amphiphilic monolayer. Langmuir 14, 7427–7434.
Templer, R.H., Seddon, J.M., Warrender, N.A., Syrykh, A., Huang, Z., Winter, R., Erbes, J., 1998b. Inverse bicontinuous cubic phases in 2:1 fatty acid/phosphatidylcholine mixtures. The effects of chain length, hydration and temperature. J. Phys. Chem. B 102, 7251–7261.
Turner, D.C., Wang, Z.G., Gruner, S.M., Mannock, D.A., McElhaney, R.N., 1992. Structural study of the inverted cubic phases of di-dodecyl alkyl-β-D-glucopyranosyl-*rac*-glycerol. J. Phys. II France 2, 2039–2063.